Science World Journal Vol. 20(No 4) 2025 https://dx.doi.org/10.4314/swj.v20i4.52
www.scienceworldjournal.org
ISSN: 1597-6343 (Online), ISSN: 2756-391X (Print)
Published by Faculty of Science, Kaduna State University

Full Length Research Article

SYNERGISTIC EFFECT OF CO-SUPPORTIVE OPEFB-MWCNT CONDUCTIVE NETWORK FOR HIGH-PERFORMANCE EMI SHIELDING APPLICATION

*[1]Ismail Ibrahim Lakin, [1]Asiya Hassan, [2]Rabi'u Abubakar Tafida, [3]Ibrahim Abubakar Alhaji

[1]Department of Physics, Faculty of Physical Sciences, Kaduna State University, Kaduna, Nigeria
[2]Department of Physics, Nigerian Defence Academy, Afaka, PMB 2109, Kaduna, Nigeria
[3]Department of Physics, Faculty of Science, Federal University of Kashere, P.M.B. 0182, Gombe, Gombe State, Nigeria

*Corresponding Author Email Address : ismaillakin59@gmail.com

ABSTRACT
The crystallinity, microstructure, complex permittivity, and electromagnetic interference (EMI) shielding effectiveness (SE) of polymeric material filled with nanofiller were investigated. The nanofiller was multiwalled carbon nanotubes (MWCNTs). In addition, the EMI SE mechanism and dielectric properties in the X-band frequency were studied. The nanocomposites were fabricated by the melt-blending method. The effect of 5-13 wt.% MWCNTs filler on the dielectric of OPEFB/PLA/MWCNTs composites was studied. It was found that 13 wt.% MWCNTs exhibited the highest EMI SE value compared to 5, 7, 9, and 11 wt.% MWCNTs.

INTRODUCTION
Currently, Electromagnetic (EM) radiation has proved to be the fourth most crucial source of public pollution, besides air, water, and noise pollution. It affects the typical behavior of systems or devices as well as is harmful to all living beings. Hence, there is an increasing demand for the development of suitable materials to attenuate the effects of the EM radiation (Cheng *et* al., 2021; Shahzad *et* al., 2016; Abbasi *et* al., 2019; Wang *et* al., 2020; Ma *et* al., 2020; Liang *et* al., 2021).
Microwave absorbers have dielectric and magnetic losses according to the type of filler used, and in general, absorption performance is dependent not only on their dielectric (permittivity) and magnetic (permeability) properties but also on the thickness and frequency. The magnetic absorbers are generally characterized by higher weight, thinner matching thickness, poor absorbing characteristics at high frequencies, and wider absorbing bandwidths in comparison with dielectric ones (Al-Saleh et al., 2013; Thomassin *et* al., 2013; Qin & Brosseau, 2012).
In developing absorbing composites, ferrites are commonly used. However, like any other metals, ferrites are heavy, corrosive, expensive, and non-biodegradable. Therefore, the use of metals such as ferrites for EMI shielding could lead to galvanic corrosion, which in turn increases the nonlinearity behavior and decreases its shielding effectiveness (Shifa *et* al., 2020; Soares *et* al., 2021). The conductive polymer has been used as an EMI shielding material for the merits of easy processing, chemical corrosion resistance, and light weight (Srivastava & Kumar, 2012; Tian *et* al., 2023).
Recently, researchers have paid close attention to polymeric nanocomposites for their enhanced electron mobility and electromagnetic absorption characteristics. EMI shielding effectiveness (SE) of the polymeric nanocomposites usually depends on the nanofiller type. Carbon nanotubes (CNTs) are one-dimensional carbon-based nanofillers with an aspect ratio, outstanding mechanical strength, and strong dielectric polarization properties that are widely employed in the field of EM shielding materials (De Volder *et* al., 2013; Ma *et* al., 2023; Wang *et* al., 2021; Lai *et* al., 2022). Among them, multi-walled carbon nanotubes (MWCNTs) have received extensive attention from researchers due to their inexpensive cost and superior processing features (Liu *et* al., 2021; Zhou *et* al., 22; Novoselov *et* al., 2013). Natural fibers have been utilized as reinforcing materials in combination with polymeric materials. Biofibers are used in polymeric composites due to their easy separation, low cost, low density, toughness, enhanced energy recovery, and significant biodegradability (Saba *et* al., 2014). The development of natural fiber composites has attracted research interest from various fields in the last few years because the fibers can replace conventional reinforcement materials in terms of weight reduction (Kumar & Sekaran, 2014). Oil palm empty fruit bunch (OPEFB) reinforced materials could reduce costs, enhance dielectric properties, thermal stability, and increase stiffness (Ahmad *et* al., 2017). Polylactic acid (PLA) is a thermoplastic polyester flexible and obtained mostly from materials that are renewable annually. PLA has high strength, elasticity modulus, stiffness, fragility, and is a biodegradable matrix (Abdalhadi *et* al., 2018). Reinforcing thermoplastics with cellulosic fibers, however, considerably increases rigidity and strength while drastically reducing composite toughness (Dike, 2022). PLA loaded with carbon nanotubes, graphite nanoplatelets, and other nanocarbons is among the best candidates for the production of structures with various sophisticated geometries through additive manufacturing (Yan *et* al., 2016).
In this study, the dielectric properties and absorption characteristics of OPEFB/PLA/MWCNTs nanocomposites were discussed. A total of 5–13 wt.% of MWCNTs filler loads were added into the OPEFB/PLA matrix to fabricate composites via the melt-blend technique and characterized at 8–12 GHz range. The electric field distributions due to material absorption were also examined. The main aim of this study was to examine the impact of various MWCNT loadings on dielectric permittivity and absorption characteristics of the OPEFB/PLA/MWCNTs nanocomposite materials.

EXPERIMENTAL
OPEFB/PLA/ MWCNTs composite preparation
The OPEFB FIBER was obtained from Bola oil mills, Ore Edo, Nigeria. To remove the wax layer of fibers, the OPEFB fibers were soaked in distilled water for 24 h. The fibers were rinsed with acetone and dried in an oven at 80 ºC for 6 h to reduce the

Science World Journal Vol. 20(No 4) 2025 https://dx.doi.org/10.4314/swj.v20i4.52
www.scienceworldjournal.org
ISSN: 1597-6343 (Online), ISSN: 2756-391X (Print)
Published by Faculty of Science, Kaduna State University

moisture. The dried fibers were crushed into powder using a crusher machine (Mailand, Hunan, China), which was then sifted 100 µm by laboratory test sieve (Endecotts, London, England). PLA was bought under the trade name polylactide resin 3052D from NatureWorks LLC (Minnetonka, MN, USA). Short MWCNTs were purchased from US Research Nanomaterials, Inc. (3302 Twig Leaf LN, Houston, TX 77084, USA) with > 95% purity. A total of 50 g of each sample was prepared for blending. The OPEFB/PLA/MWCNTs composites were fabricated by mixing 6%, 10%, 14%, 18%, and 22% mass percentages of MWCNTs with OPEFB fiber and PLA at a fixed ratio of 3:7. The PLA was melted in a Brabender Internal Mixer for 2 min at 150 ºC with 50 rpm of rotor speed. Then the OPEFB fiber and MWCNTs powders were added and continued blending for another 12 min. The compression of the composites was done using the hydraulic hot press at 120 ºC molding temperature, 150 kg/cm^2 pressure, for 10 min, (as illustrated in Figure 1) then cooled at 30 ºC for 10 min.

Figure 1. Fabrication of OPEFB/PLA/MWCNTs composites

Characterizations

X-Ray Diffraction (XRD)

The crystallinity of PLA, OPEFB, and OPEFB?PLA/MWCNTs composites were analyzed using a Shimadzu XRD 600 diffractometer (Tokyo, Japan) with a nickel-filtered Cu- Kα (λ = 0.1542 nm) beam at a voltage of 30 kV and a current of 30 mA. The composites were examined with a scanning rate of 2º /min at 25 ºC within a 2 theta range of 10º to 80º.

Field Emission Scanning Electron Microscopy (FE-SEM)

The morphology of the samples (PLA, OPEFB, and OPEFB/PLA/MWCNTs) were examined using FE-SEM (Nova NanoSEM 230, FEI Holland) at a fixed voltage of 10 kV. The samples were coated with gold using a Bio-Rad (Hercules, CA, USA) coating system and then dried in an oven for 30 min to provide better conductivity.

Dielectric Properties Measurement

The measurements for the complex permittivity of the composites were carried out using the open-ended coaxial (OEC) probe. The probe was connected to an Agilent Network Analyser (VNA, Agilent Technologies, CA, USA) via a high-precision coaxial test cable (Mensah *et* al., 2019). A standard one-port, short-air-water calibration was performed, and a reference standard material (Polytetrafluoroethylene) was characterized to validate the accuracy of the calibration. As illustrated in Figure 2, the OEC probe was then firmly positioned on the flat surface of the samples to determine complex permittivity using the software installed on the VNA. All the measurements were performed at a frequency range of 8-12 GHz.

Figure 2. Complex Permittivity measurement using open-ended coaxial probe.

Measurement of Scattering Parameters (S-parameters)

The S-parameters were measured using a microstrip line (6 × 5) cm^2 in dimension connected to an HP8720B VNA through the two-port configuration as shown in Figure 3. The measurements were performed at a frequency range from 8 to 12 GHz. The composites to be measured were covered with a copper foil in order to avoid dispersion of radiation excited through the composite. Firm contact was ensured between the composite base and the microstrip line to avoid air gap during the measurement (Giita *et* al., 2012).

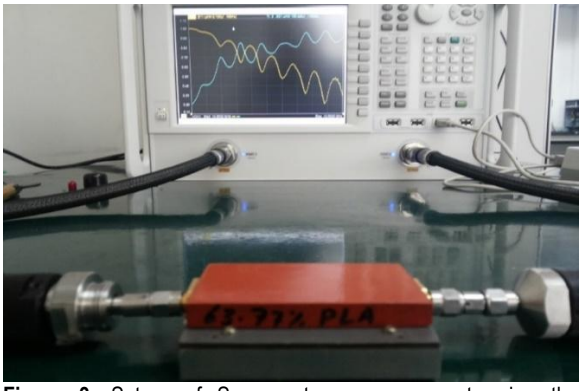

Figure 3. Set-up of S-parameters measurement using the microstrip sensor.

RESULTS AND DISCUSSION

X-Ray Diffraction (XRD) Analysis

The OPEFB, PLA, MWCNTs, and OPEFB/PLA/MWCNTs composites were characterized to study the effect of MWCNTs on the OPEFB/PLA composites' crystallinity. As presented in Figure 4, the XRD patterns of pure PLA showed a wide diffraction peak of approximately 2θ ≈ 18°. The PLA showed no characteristic peak and indicated that PLA has an amorphous structure (Challabi *et* al., 2019). The OPEFB also exhibits peaks at 2θ ≈ 16° and 2θ ≈ 24°, indicating amorphous and crystalline regions (Harun *et* al., 2013). Cellulosic natural fibers contain both crystalline (ordered) and amorphous (disordered). Thus, the existence of dual features in the fiber is consistent with the presence of ordered and disordered regions (Ali *et* al., 2015). The broad peaks of OPEFB suggest a carbon-based and cellulose-type material (Abdalhadi *et* al., 2018).

Science World Journal Vol. 20(No 4) 2025 https://dx.doi.org/10.4314/swj.v20i4.52
www.scienceworldjournal.org
ISSN: 1597-6343 (Online), ISSN: 2756-391X (Print)
Published by Faculty of Science, Kaduna State University

The MWCNTs XRD pattern displays a wide diffraction peak at 2θ ≈ 26.2° that corresponds to (002) and a small peak at 2θ ≈ 44.2° corresponding to (100), indicating the crystalline structure of MWCNTs (Bibi *et* al., 2017). Moreover, the OPEFB/MWCNTs nanocomposites showed characteristic diffraction peaks at 2θ ≈ 26.2° and 2θ ≈ 44.2°. The high diffraction peak at 26.2° may be due to the MWCNTs stacking layers with the disorder (002) (Ahmad *et* al., 2025).

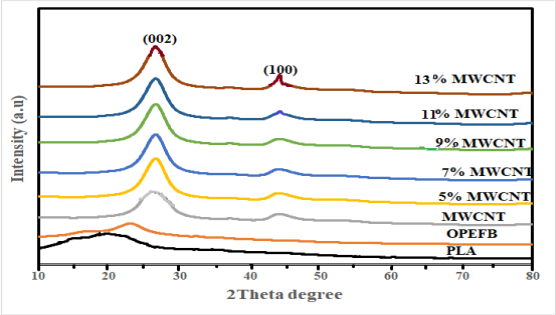

Figure 4. XRD pattern of OPEFB, PLA, MWCNTs, and OPEFB/PLA/MWCNTs composites with different concentrations of MWCNTs.

Field emission scanning electron microscopy (FE-SEM) Analysis

The FE-SEM images in Figure 4a, b showed the morphology of OPEFB/PLA/5wt. % MWCNTs and OPEFB/PLA/13wt. % MWCNTs nanocomposites. The MWCNTs bind strongly to the OPEFB/PLA matrix surface and tips due to the effectiveness of the Brabender mixer as can be seen in the FESEM images. The uniform dispersion of the hybrid filler particles in polymer systems leads to the creation of a co-supportive network that is likely to strengthen composite electrical conductivity. Nanocomposite's network structure with a high available surface area is expected to contribute to various interfacial polarization resulting in the weakening of the EM waves (Ravindren *et* al., 2019).

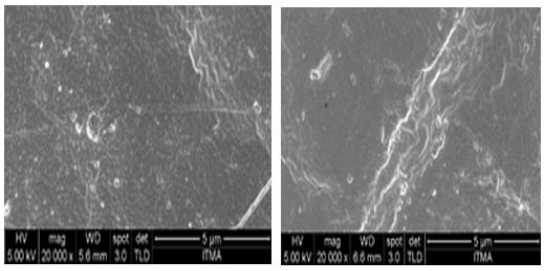

(a) (b)

Figure 4. FE-SEM images of (a) OPEFB/PLA/5% MWCNTs (b) OPEFB/PLA/13% MWCNTs

Dielectric Properties Analysis

Figure 5 displays the complex permittivity of the OPEFB fibers and MWCNTs and the frequency variation. Generally, dielectric constant (ε') and loss factor (ε") values of both OPEFB fiber and MWCNTs decreased with frequency increase, as described by the Maxwell Wenger polarization model (Maleknejad *et* al., 2016). The MWCNTs had higher ε' and ε" values in the 8-12 GHz range than the OPEFB fiber. The OPEFB fiber and MWCNTs ε' values were 3.57 and 7.65, while the ε" values were 0.63 and 1.24, respectively.

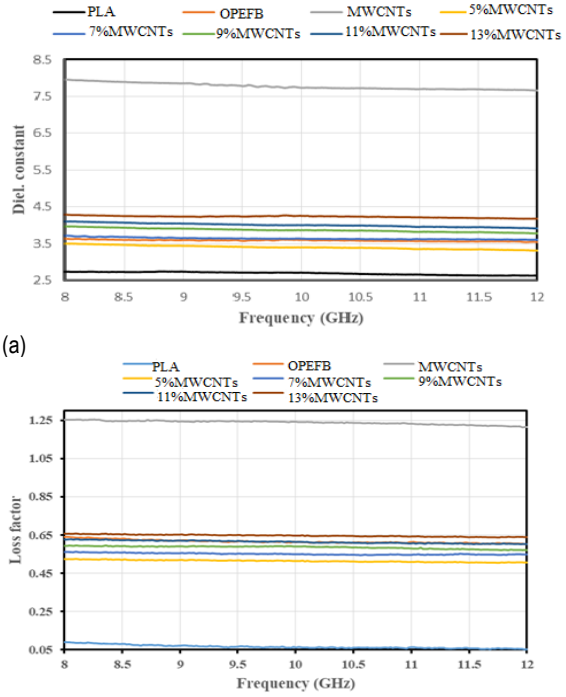

Figure 5. variation in: (a) dielectric constant and (b) loss factor of OPEFB/PLA/MWCNTs

The effect of the 5-13 wt.% MWCNTs filler on the dielectric of OPEFB/PLA/MWCNTs composites was studied, and the variation in ε' and ε" values in the range 8-12 GHz is shown in Figure 5. It has been reported that the quality of conductive fillers distributed in a polymer matrix will play a significant role in the entire sample's dielectric behaviors (Mensah *et* al., 2019). PLA has low permittivity because the small amount of macromolecular polarization. The values of ε' and ε" in the 8-12 GHz range decreased with frequency for the 5-13 wt.% composites. The complex permittivity values for the composites depend primarily on the contribution of interfacial, orientation, and electronic and atomic polarization in the material, due to the differences in the polarization or conductivity of the matrix and the filler. The results show that the complex permittivity of OPEFB/PLA composites can be increased significantly by the addition of MWCNTs.

Material Reflectance and Absorbance Loss

The S-parameters (S_{11} and S_{21}) can be conveniently correlated with reflectance (R) and transmittance (T), where,

$$T = \left|\frac{E_T}{E_I}\right|^2 = |S_{21}|^2 \quad (3.1)$$

$$R = \left|\frac{E_R}{E_I}\right|^2 = |S_{11}|^2 \quad (3.2)$$

Giving absorbance (A) as,

$$A = (1 - T - R) \quad (3.3)$$

$$A = (1 - |S_{21}|^2 - |S_{11}|^2 \quad (3.4)$$

SE_A can be determined by the following equations;

$$SE_A = -10log_{10}\left(\frac{T}{1-R}\right) \quad (3.5)$$

The microstrip is a free-space technique where waves can radiate at the input and output as well as along the sample. The variation of the absorption (SE_A) component of the EMI shielding against the frequency for the OPEFB-PLA-MWCNTs composites is shown in Figure 6. The SE_A values of the composites increased across the 8-12 GHz. The increment ranges from 3.06 at 8 GHz to 9.91 dB at 11.85 GHz. There is no substantial variation in the values of SE_A, considering 5 to 13 wt.% composites. This small variation is probably due to measurement uncertainties during the permittivity measurements. These findings demonstrate that the OPEFB-PLA-MWCNTs are capable of significant microwave absorption and should act as a cheaper and more effective option for applications throughout the investigated frequency range.

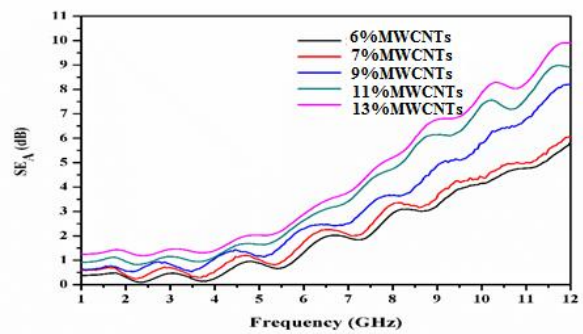

Figure 6. Variation in absorption loss (SE_A) for the OPEFB-PLA-MWCNTs nano composites

Conclusion

The composite material consisting of OPEFB fiber, PLA, and MWCNTs was successfully synthesized via the melt-blend technique. XRD analysis reveals that the increasing addition of MWCNTs in the composite will result in the increase in slight increase in the relative intensity due to the MWCNTs stacking layers with the disorder (002). FESEM micrographs show that the MWCNTs bind well with the OPEFB/PLA matrix. Electromagnetic measurement reveals promising values of EMI shielding effectiveness through absorption. The increase in MWCNTs results in the enhanced performance of the shielding effectiveness.

REFERENCES

Abdalhadi, D. M., Abbas, Z., Ahmad, A. F., Matori, K. A., & Esa, F. (2018). Controlling the properties of OPEFB/PLA polymer composite by using Fe2O3 for microwave applications. *Fibers and Polymers*, *19*(7), 1513-1521.

Abbasi, H., Antunes, M., & Velasco, J. I. (2019). Recent advances in carbon-based polymer nanocomposites for electromagnetic interference shielding. *Progress in Materials Science*, *103*, 319-373.

Ahmad, A. F., Abbas, Z., Obaiys, S. J., & Abdalhadi, D. M. (2017). Improvement of dielectric, magnetic and thermal properties of OPEFB fibre–polycaprolactone composite by adding Ni–Zn ferrite. *Polymers*, *9*(2), 12.

Ahmad, J., Maryam, A., Manzoor, H. S., Nasir, N., Nawab, Y., & Ahmad, H. S. (2025). Enhancement of EMI shielding effectiveness in carbon fiber-reinforced composite structures impregnated with MWCNT and Fe2O3 nanofillers through optimized laminating sequences. *Materials Science and Engineering: B*, *313*, 117980.

Ali, M. E., Yong, C. K., Ching, Y. C., Chuah, C. H., & Liou, N. S. (2015). Effect of single and double stage chemically treated kenaf fibers on mechanical properties of polyvinyl alcohol film. *BioResources*, *10*(1), 822-838.

Al-Saleh, M. H., Saadeh, W. H., & Sundararaj, U. (2013). EMI shielding effectiveness of carbon based nanostructured polymeric materials: a comparative study. *carbon*, *60*, 146-156.

Bibi, M., Abbas, S. M., Ahmad, N., Muhammad, B., Iqbal, Z., Rana, U. A., & Khan, S. U. D. (2017). Microwaves absorbing characteristics of metal ferrite/multiwall carbon nanotubes nanocomposites in X-band. *Composites Part B: Engineering*, *114*, 139-148.

Challabi, A. J. H., Chieng, B. W., Ibrahim, N. A., Ariffin, H., & Zainuddin, N. (2019). Effect of Superheated Steam Treatment on the Mechanical Properties and Dimensional Stability of PALF/PLA Biocomposite. *Polymers*, *11*(3), 482.

Cheng, Y., Li, X., Qin, Y., Fang, Y., Liu, G., Wang, Z., ... & Ye, M. (2021). Hierarchically porous polyimide/Ti3C2T x film with stable electromagnetic interference shielding after resisting harsh conditions. *Science advances*, *7*(39), eabj1663.

De Volder, M. F., Tawfick, S. H., Baughman, R. H., & Hart, A. J. (2013). Carbon nanotubes: present and future commercial applications. *science*, *339*(6119), 535-539.

Dike, A. S. (2022). Improvement of mechanical and physical performance of poly (lactic acid) biocomposites by application of surface silanization for huntite–hydromagnesite mineral. *Journal of Thermoplastic Composite Materials*, *35*(8), 1061-1075.

Giita Silverajah, V. S., Ibrahim, N. A., Yunus, W. M. Z. W., Hassan, H. A., & Woei, C. B. (2012). A comparative study on the mechanical, thermal and morphological characterization of poly (lactic acid)/epoxidized palm oil blend. *International journal of molecular sciences*, *13*(5), 5878-5898.

Harun, N. A. F., Baharuddin, A. S., Zainudin, M. H. M., Bahrin, E. K., Naim, M. N., & Zakaria, R. (2013). Cellulase Production from Treated Oil Palm Empty Fruit Bunch Degradation by Locally Isolated Thermobifida fusca. *BioResources*, *8*(1).

Kumar, K. P., & Sekaran, A. S. J. (2014). Some natural fibers used in polymer composites and their extraction processes: a review. *Journal of Reinforced Plastics and Composites*, *33*(20), 1879-1892.

Lai, M. F., Huang, C. H., Lou, C. W., Chuang, Y. C., Wei, C. Y., & Lin, J. H. (2022). Multi-walled carbon nanotubes/polypropylene-based coating layer on the composite metal filaments: Characteristic evaluations and radiation-shielded fabric. *Fibers and Polymers*, *23*(3), 768-774.

Liang, C., Gu, Z., Zhang, Y., Ma, Z., Qiu, H., & Gu, J. (2021). Structural design strategies of polymer matrix composites for electromagnetic interference shielding: a review. *Nano-micro letters*, *13*(1), 181.

Liu, D., Kong, Q. Q., Jia, H., Xie, L. J., Chen, J., Tao, Z., ... & Chen, C. M. (2021). Dual-functional 3D multi-wall carbon nanotubes/graphene/silicone rubber elastomer: Thermal management and electromagnetic interference shielding. *Carbon*, *183*, 216-224.

Ma, R. Y., Yi, S. Q., Li, J., Zhang, J. L., Sun, W. J., Jia, L. C., ... & Li, Z. M. (2023). Highly efficient electromagnetic interference shielding and superior mechanical performance of carbon nanotube/polydimethylsiloxane composite with interface-reinforced segregated structure. *Composites Science and Technology*, *232*, 109874.

Ma, Z., Kang, S., Ma, J., Shao, L., Zhang, Y., Liu, C., ... & Gu, J. (2020). Ultraflexible and mechanically strong double-layered aramid nanofiber–Ti3C2T x mxene/silver nanowire nanocomposite papers for high-performance electromagnetic interference shielding. *ACS nano*, *14*(7), 8368-8382.

Maleknejad, Z., Gheisari, K., & Raouf, A. H. (2016). Structure, microstructure, magnetic, electromagnetic, and dielectric properties of nanostructured Mn–Zn ferrite synthesized by microwave-induced urea–nitrate process. *Journal of superconductivity and novel Magnetism*, *29*(10), 2523-2534.

Mensah, E. E., Abbas, Z., Azis, R. A. S., & Khamis, A. M. (2019). Enhancement of Complex Permittivity and Attenuation Properties of Recycled Hematite (α-Fe2O3) Using Nanoparticles Prepared via Ball Milling Technique. *Materials*, *12*(10), 1696.

Novoselov, K. S., Geim, A. K., Morozov, S. V., Jiang, D. E., Zhang, Y., Dubonos, S. V., ... & Firsov, A. A. (2004). Electric field effect in atomically thin carbon films. *science*, *306*(5696), 666-669.

Qin, F., & Brosseau, C. (2012). A review and analysis of microwave absorption in polymer composites filled with carbonaceous particles. *Journal of applied physics*, *111*(6).

Ravindren, R., Mondal, S., Nath, K., & Das, N. C. (2019). Synergistic effect of double percolated co-supportive MWCNT-CB conductive network for high-performance EMI shielding application. *Polymers for Advanced Technologies*, *30*(6), 1506-1517.

Saba, N., Md Tahir, P., & Jawaid, M. (2014). A review on potentiality of nano filler/natural fiber filled polymer hybrid composites. *Polymers*, *6*(8), 2247-2273.

Shahzad, F., Alhabeb, M., Hatter, C. B., Anasori, B., Man Hong, S., Koo, C. M., & Gogotsi, Y. (2016). Electromagnetic interference shielding with 2D transition metal carbides (MXenes). *Science*, *353*(6304), 1137-1140.

Shifa, M., Tariq, F., Khan, F., Toor, Z. S., & Baloch, R. A. (2020). Towards light weight multifunctional hybrid composite housing for satellite electronics. *Materials Research Express*, *6*(12), 125629.

Soares, B. G., Barra, G. M., & Indrusiak, T. (2021). Conducting polymeric composites based on intrinsically conducting polymers as electromagnetic interference shielding/microwave absorbing materials—A review. *Journal of Composites Science*, *5*(7), 173.

Srivastava, S. K., & Manna, K. (2022). Recent advancements in the electromagnetic interference shielding performance of nanostructured materials and their nanocomposites: a review. *Journal of Materials Chemistry A*, *10*(14), 7431-7496.

Thomassin, J. M., Jerome, C., Pardoen, T., Bailly, C., Huynen, I., & Detrembleur, C. (2013). Polymer/carbon based composites as electromagnetic interference (EMI) shielding materials. *Materials Science and Engineering: R: Reports*, *74*(7), 211-232.

Tian, K., Hu, D., Wei, Q., Fu, Q., & Deng, H. (2023). Recent progress on multifunctional electromagnetic interference shielding polymer composites. *Journal of Materials Science & Technology*, *134*, 106-131.

Wang, L., Song, P., Lin, C. T., Kong, J., & Gu, J. (2020). 3D shapeable, superior electrically conductive cellulose nanofibers/Ti3C2Tx MXene aerogels/epoxy nanocomposites for promising EMI shielding. *Research*.

Wang, Y. Y., Sun, W. J., Yan, D. X., Dai, K., & Li, Z. M. (2021). Ultralight carbon nanotube/graphene/polyimide foam with heterogeneous interfaces for efficient electromagnetic interference shielding and electromagnetic wave absorption. *Carbon*, *176*, 118-125.

Yan, L., Kasal, B., & Huang, L. (2016). A review of recent research on the use of cellulosic fibres, their fibre fabric reinforced cementitious, geo-polymer and polymer composites in civil engineering. *Composites Part B: Engineering*, *92*, 94-132.

Zhou, J., Tao, H., Xia, L., Zhao, H., Wang, Y., Zhan, Y., & Yuan, B. (2022). An innovative ternary composite paper of graphene and Fe3O4 decorated multi-walled carbon nanotube for ultra-efficient electromagnetic interference shielding and fire-resistant properties. *Composites Communications*, *32*, 101181.